

## Utility of Single Shot Fast Spin Echo Technique in Evaluating Pancreaticobiliary Diseases : T2-weighted Image and Magnetic Resonance Cholangiopancreatography<sup>1</sup>

Byoung Wook Choi, M.D., Myeong-Jin Kim, M.D., Jae Bok Chung, M.D.<sup>2</sup>,  
Heung Kyu Ko, M.D., Dong Joon Kim, M.D., Joo Hee Kim, M.D.,  
Jae-Joon Chung, M.D., Hyung Sik Yoo, M.D., Jong Tae Lee, M.D.

**Purpose :** To evaluate the accuracy of T2-weighted imaging and MR cholangiopancreatography using the single shot fast spin-echo technique for evaluating pancreaticobiliary disease.

**Materials and Methods :** Between March and July 1997, axial and coronal T2-weighted images (TE:80-200 msec) and MR cholangiopancreatograms (TE:800-1200 msec) were obtained in two ways [single slab (thickness:30-50 mm) and multislice acquisition under chemical fat saturation] using SSFSE pulse sequencing in 131 cases of suspected pancreaticobiliary disease. The accuracy of SSFSE MR imaging was assessed in 89 lesions of 74 patients [male,48; female,26; age range,30-86 (mean,59)years] confirmed surgicopathologically (50 lesions in 39 patients) and clinically (39 lesions in 35 patients). Two radiologists reviewed the MR images and diagnosis was determined by consensus.

**Results :** Correct diagnosis was confirmed in 84 of 89 lesions (94%). Seven lesions were falsely interpreted, false positive and false negative results accounting for two and five cases, respectively. Two pancreatic cancers were misdiagnosed as pancreatitis and a cancer of the proximal common bile duct (CBD) was interpreted as a distal CBD cancer. The sensitivity of SSFSE MR imaging for malignancy was 93%. One CBD stone revealed by endoscopic retrograde cholangiopancreatography (ERCP) was not detected on MR images. In contrast, a stone in the CBD seen on MR images was not apparent on subsequent ERCP. Sensitivity and specificity for calculous disease were 96% and 99.7%, respectively. A benign stricture of the ampulla of Vater was falsely interpreted as normal, and correct diagnosis was possible in two falsely diagnosed cases when MR images were reviewed retrospectively.

**Conclusion :** The combination of T2-weighted and cholangiographic images using SSFSE is an accurate method for diagnosing pancreaticobiliary diseases.

**Index words :** Magnetic resonance (MR), half-Fourier imaging

Bile ducts, MR

Bile ducts, stenosis or obstruction

Pancreatic ducts, MR

Magnetic resonance (MR), rapid imaging

<sup>1</sup>Department of Diagnostic Radiology & Research institution of Radiological Science

<sup>2</sup>Department of Internal Medicine, Division of Gastroenterology Yonsei University College of Medicine (HMP-96-M-2-1019)

Received March 15, 1999 ; Accepted June 1, 1999

Address reprint requests to : Myeong-Jin Kim, M.D., Department of Diagnostic Radiology, Severance Hospital, Yonsei University College of Medicine, #134, Shinchon-dong, Seodaemun-du Seoul 120-752, Korea.

Tel. 82-2-361-5837 Fax. 82-2-393-3035

The recently-introduced single shot fast spin echo (SS-FSE) or half-Fourier single shot turbo spin echo (HASTE) technique, using a single refocusing pulse and half-Fourier acquisition, shortens acquisition time to 2-20 seconds. For cholangiopancreatographic imaging of pancreaticobiliary diseases, most patients can hold their breath for this length of time. In terms of image-degradation due to motion during MR imaging, which is the major problem in MR imaging of pancreaticobiliary tracts, breath-hold MR cholangiopancreatography (MR-CP) using single shot half-Fourier acquisition provides good quality images free from motion artifact. Several investigators (1-6) have reported the superiority of this technique to previously-introduced sequences for MR-CP including two- or three-dimensional steady state free precession (SSFP)(7-11) and fast spin echo techniques (12-22) with or without the breath-hold technique. MR-CP using single shot half-Fourier acquisition can accurately depict normal structures and the presence and level of biliary obstruction without motion artifact and can, according to Regan et al. (4), be performed even in uncooperative and those who are ill.

T2-weighted images acquired using a relatively short echo time and without chemical fat saturation provide more detail of soft tissue than source images acquired for MIP (maximal intensity projection) reconstruction using a long echo time and chemical fat saturation. Although source images for MIP reconstruction have been reported by Yamashita et al. (6) to provide the best evaluation of stones in biliary trees, T2-weighted image can take the place of source images.

In many institutes, MRCP has been used to complement endoscopic retrograde cholangiopancreatography (ERCP) or even routinely for the evaluation of pancreaticobiliary diseases. Because of its advantages of noninvasiveness, virtually no procedure-related mortality or morbidity, and visualization of the duct proximal to complete obstruction - especially when therapy is not anticipated - MRCP rather than ERCP is recommended. T2-weighted images without fat saturation can be obtained in a relatively short period of time using a SSFSE sequence in addition to MRCP. The two techniques in combination are believed to provide a more accurate diagnosis as well as suggesting the next step in diagnosis and treatment. In patients with pancreaticobiliary diseases we evaluated the diagnostic accuracy of MRCP and T2-weighted images acquired using a SSFSE sequence.

## Materials and Methods

Between March and July 1997, T2 weighted images and MR cholangiopancreatograms were obtained using SSFSE pulse sequence in 131 cases of suspected pancreaticobiliary disease. The accuracy of SSFSE MR imaging was assessed in 89 lesions of 74 patients [men, 48; women, 26; age range, 30-86 (mean age, 59) years] confirmed surgicopathologically (50 lesions in 39 patients) or clinically by ultrasonography, CT scanning, or direct cholangiography including ERCP (39 lesions in 35 patients, Table 1). The Remaining 47 patients were excluded due to insufficient additional information or too short a period of follow-up. Using a 1.5-T system (Horizon, GE, Milwaukee, Wis., USA) and a phased-array torso coil, MR images were obtained. For coronal localizer images, single-shot fast spin-echo with a slice thickness of 8-10 mm and a slice gap of 0-2 mm with effective TE of 85-95 msec, phase encoding of 192, frequency encoding of 256, and receiver bandwidth of 31.3 kHz were used. Axial and coronal T2-weighted images were obtained using the fol-

Table 1. Clinically Diagnosed Cases (n= 35)

Diagnostic Modalities	Diseases	Total
CT, US (n= 7)	Bile duct cancer(1)	11
	GB cancer(1)	
	Extrahepatic duct stone(3)	
	Intrahepatic duct stone(3)	
	GB stone(2)	
CT, ERCP (n= 9)	Recurrent pyogenic cholangitis(1)	10
	Bile duct cancer(4)	
	Pancreas cancer(2)	
	Extrahepatic duct stone(1)	
	Intrahepatic duct stone(1)	
CT (n= 6)	pancreatic duct stone(2)	6
	Bile duct cancer(2)	
	GB cancer(1)	
US (n= 5)	Pancreas cancer(1)	5
	Extrahepatic duct stone(2)	
	Bile duct cancer(1)	
	Liver malignancy(1)	
ERCP (n= 2)	Serous cystadenoma of pancreas(1)	2
	Adenomyomatosis of GB(1)	
	Ampullary cancer(1)	
CT, US, ERCP (n= 2)	Extrahepatic duct stone(1)	2
	Bile duct cancer(1)	
US, ERCP (n= 1)	Mucinous tumor of pancreas(1)	1
	Bile duct cancer(1)	
US, PTC (n= 1)	Bile duct cancer(1)	1
PTC (n= 1)	Intrahepatic duct stone(1)	1
Total		39

The number in parenthesis is the number of lesions.

lowing parameters; TE, 80-200 msec; matrix size, 256 × 256; thickness, 5 mm without gap. FOV was applied between 24 cm and 36 cm according to a patient's body habitus and expected extent of pathology based on the image for localization. Between eight and fourteen images were acquired within 30 seconds, with 80% of these within 20 seconds. MRCP was performed in two ways, single slab and multislice acquisition under chemical fat saturation. Single slab image was obtained in the coronal plane with a TE of 800-1200 msec, thickness of 30-50 mm, FOV of 28 cm, and matrix size of 256 × 256. Acquisition time never exceeded two seconds. Multislice acquisition employed the same parameters as single slab acquisition except for a thickness of 3-5 mm without gap. For the reconstruction of maximal intensity projection (MIP) images, multislice images were transferred to a workstation. MIP images were reconstructed in their anterior-posterior perspective and rotated for up to 45 degrees towards the left and right with an interval of 15 degrees. No antiperistaltic or paramagnetic agent was used.

Using clinical information, two abdominal radiologists read the MR images and a diagnosis was determined by consensus. Calculi were considered present when a round, oval, or multiangular signal void was seen within the lumen of bile ducts. To calculate diagnostic accuracy for calculous disease, five locations - namely the intrahepatic, extrahepatic, cystic, and pancreatic duct, and the gallbladder (total 74 × 5 = 370 locations) - were checked

for the presence of a stone. Malignancy was diagnosed when a definite mass was visible with or without narrowing or obstruction. To determine the accuracy with which malignancy was diagnosed, its origin was recorded in four categories: the bile duct, pancreas, gallbladder, and 'other'. Direct extension into adjacent organs was not included as a separate diagnosis. In cases of stenosis without a definite visible mass, abrupt narrowing, asymmetry, shouldering, or a combination of these findings was used to determine the cause of obstruction. Because many patients were 'missing' and thus had not been followed up, or because no confirmative diagnosis was available in clinically equivocal cases, pancreatitis was not included in this study. Mucinous neoplasm of the pancreas was classified as a miscellaneous disease rather than a malignancy. Mirizzi syndrome and recurrent pyogenic cholangiohepatitis were considered as separate diagnoses in addition to a diagnosis of calculi. Other miscellaneous diseases were diagnosed using the same criteria as those used in conventional CT and direct cholangiography.

## Results

Using MR cholangiography and T2 weighted images, diagnosis was correct in 84 of 89 lesions (94%). Seven lesions were falsely interpreted, two cases being false positive and five false negative. Among the former, one

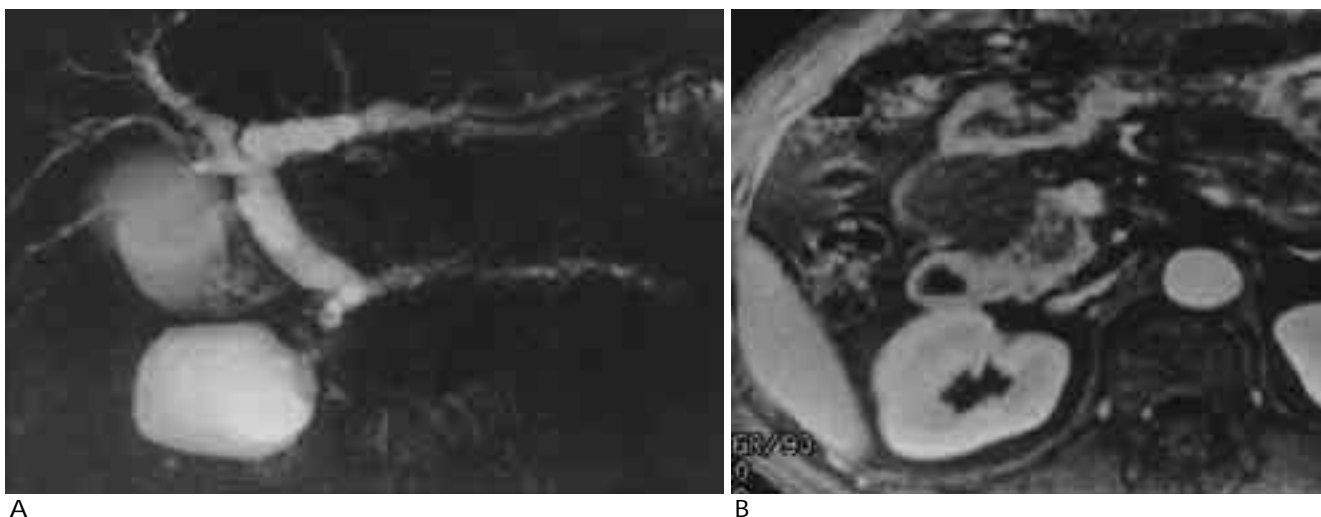


Fig. 1. Pancreas cancer with pseudocyst

A. Single projection image shows a well demarcated large cystic mass on the right of the pancreas head portion. Diffuse dilatation of pancreas duct and common bile duct is noted.

B. Gadolinium-enhanced T1-weighted axial image shows no definite mass lesion in the pancreas head except for a suspicious poorly enhancing portion. One month later, jaundice was aggravated acutely and follow-up CT scan shows a definite poorly enhanced bulging mass in the head of the pancreas. Previously noted suspicious poorly enhancing portion of the pancreas head was postulated as the missing mass lesion retrospectively.

case was thought to be malignant and in the other a calculus was thought to be present, while among the latter, three malignant and two benign cases were misinterpreted.

Among 20 bile duct cancers, one case of proximal common duct cancer was misdiagnosed on the basis of MR images as distal common duct cancer and was counted as both a false positive for the distal CBD and a false negative for the proximal lesion. Two of nine pancreatic cancers (sensitivity 78 %) were misdiagnosed simply as pancreatitis. On the basis of MR images, one of these cases was initially thought to be pancreatitis with a pseudocyst but without a definite mass lesion (Fig. 1). Retrospective review of MR images, however, revealed a suspicious lesion with low signal intensity and without bulging contour or ductal abnormality in the head of the pancreas. The other cases were falsely diagnosed because of its small size (11 mm), the absence of mass effect and associated ductal abnormality seen on MRCP and T2-weighted images using SSFSE sequencing. Ampullary carcinoma in six patients (sensitivity 100 %) was correctly diagnosed on the basis of MR images (Fig. 2). Six cases of gallbladder carcinoma, all of which were correctly diagnosed (sensitivity 100 %), had visible masses with definite invasion of adjacent organs, especially the liver. One case of duodenal malignancy and three of liver malignancy were correctly diagnosed. The sensitivity of SSFSE MR imaging for malignancy was 93%(42/45) (Table 1).

Of the 89 lesions, 25 lesions (28 %) were calculous, and among these, extrahepatic duct stones were found in seven (28 %) (Fig. 3). Two cases of extrahepatic duct stone were misdiagnosed, one as false positive and one as false negative (Fig. 4). Intrahepatic duct stones were correctly diagnosed in nine patients. Four of these had CBD stones simultaneously, and in four others stones were present in the left hepatic duct (Fig. 5). In the other case, stones were located in the right hepatic duct, mainly in the posterior segment. In three of four patients with



Fig. 2. Ampullary tumor. Note a distal round dark-signal obstructive mass (arrow) in MRCP.

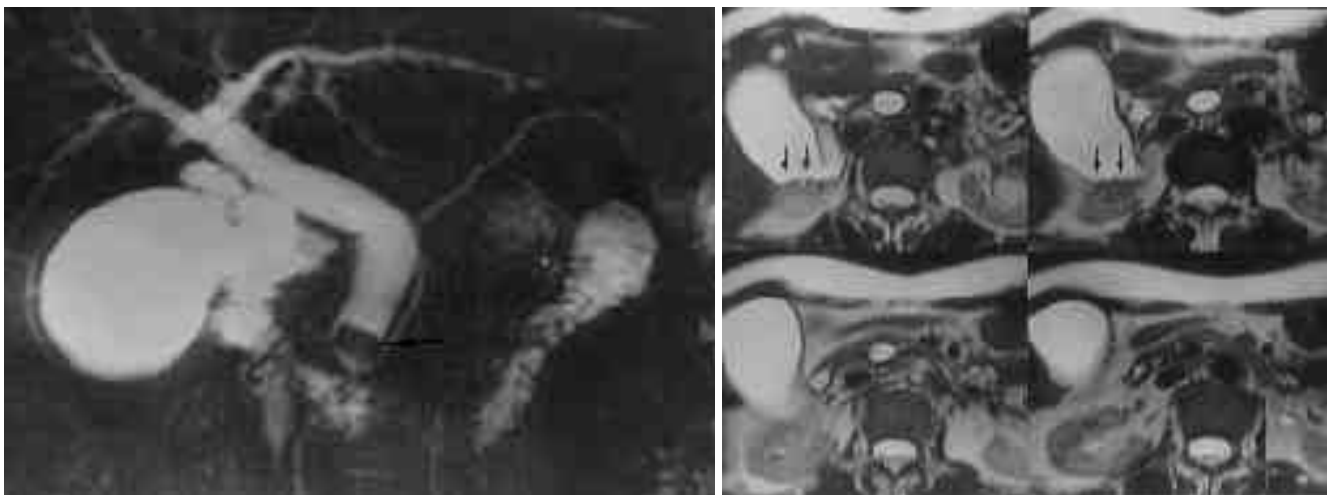


Fig. 3. Distal common bile duct stone and gallstones.  
 A. A rectangular-shaped calculus (arrow) is surrounded by bright signal of bile in the distal common bile duct on single projection image.  
 B. T2-weighted axial images show multiple small stones (arrows) in the dependent portion of the gallbladder, which was not detected, in single projection coronal image.

stones in the left hepatic duct, recurrent pyogenic cholangitis with associated ductal dilatation and parenchymal atrophy of adjacent liver was diagnosed. Three of four cases of recurrent pyogenic cholangitis were confirmed and surgically treated; the other patient underwent both CT scanning and ultrasonography. Six patients with GB stones and one with a cystic duct stone were correctly diagnosed. Five of six patients with GB stones had other disease entities concurrently: a CBD stone in three cases, Mirizzi syndrome in one (Fig. 6), and hilar cholangiocarcinoma in one. All these five cas-

es were correctly interpreted. Pancreatic duct stone was correctly diagnosed in two patients, one of whom showed a round signal void lesion, 1 cm in diameter, in the head portion of the main pancreatic duct and another 0.7 cm signal void lesion in the body portion with dilatation of the main and side branches of the pancreatic duct. The other patient showed irregular tortuous dilatation of the pancreatic duct with a 1 cm round signal void lesion in the head portion and multiple filling defects measuring 3-6 mm. Sensitivity and specificity for calculous disease were 96 % (24/25) and 99.7 % (344/345), re-



Fig. 4. False positive of choledocholithiasis. A sharply demarcated polygonal-shaped signal void lesion (arrow) is noted in the lumen of the mid portion of the common bile duct on T2-weighted coronal image. No calculus was demonstrated in the previous ERCP and no further evaluation was performed for confirmation.

Table 2. Malignant Biliary or Pancreatic Ductal Obstruction (n= 45) on MRCP

	Correct Diagnosis	Incorrect Diagnosis
Bile duct cancer	19	2*
Pancreas cancer	7	2
Ampullary cancer	6	-
GB cancer	6	-
Duodenal Cancer	1	-
Liver malignancy	3	-

\* : One case is a false positive.

Table 3. Calculous Disease (n= 25) on MRCP

	Correct Diagnosis	Incorrect Diagnosis
Extrahepatic duct	6	2*
Intrahepatic duct	9	-
GB, cytic duct	7	-
Pancreatic duct	2	-

\* : One case is a false positive.

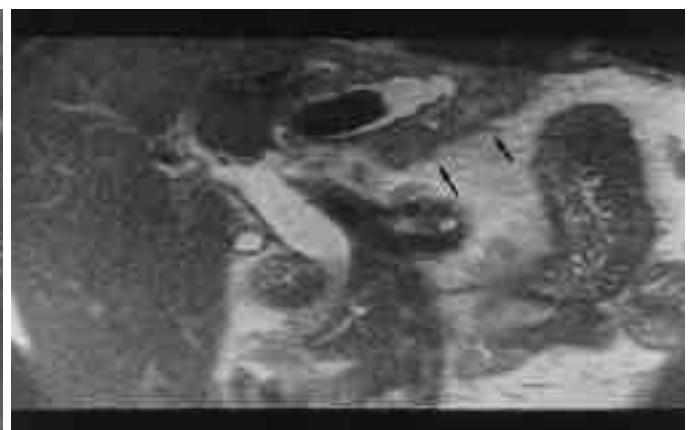


Fig. 5. Recurrent pyogenic cholangitis with left intrahepatic duct stone.  
 A. Single projection MR image clearly shows multiple variable-sized signal void lesions (arrows) in the dilated left intrahepatic duct. However, surrounding liver parenchyma cannot be evaluated.  
 B. In contrast to the single projection image, T2-weighted coronal image shows atrophied surrounding liver parenchyma (arrows) with increased signal intensity compared with normal parenchyma of the right lobe of the liver. Recurrent pyogenic cholangitis was confirmed by left lobectomy.

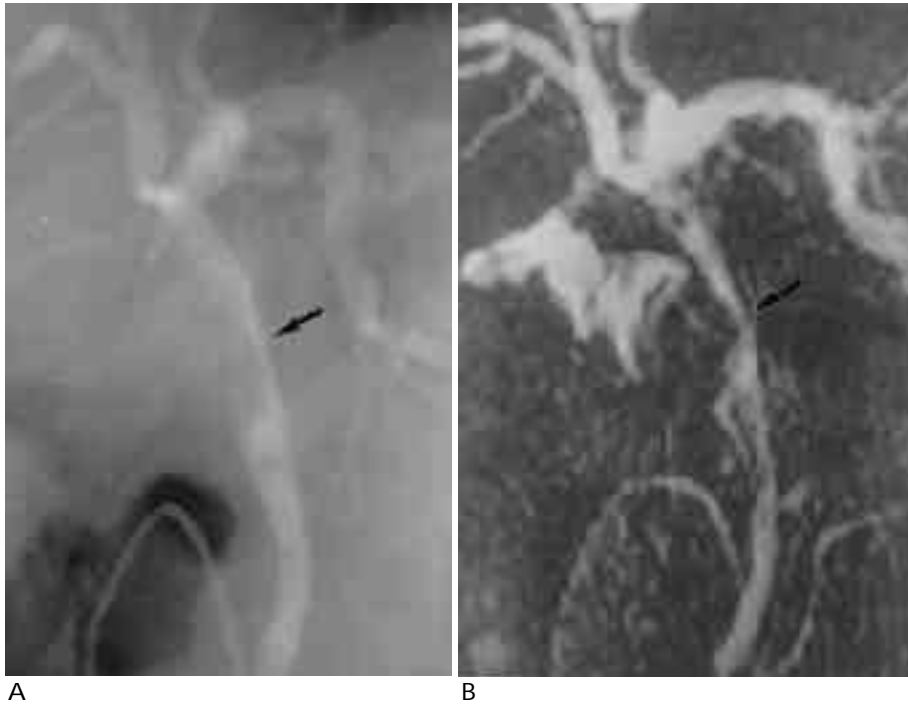


Fig. 6. Mirizzi syndrome  
 A. ENBD Cholangiogram, B. MRCP-single projection, C. T2-weighted image. Irregular indentation on proximal common bile duct (arrow) is seen on cholangiographic images in A. B. Proximal CBD cancer was suggested on the ENBD cholangiogram. MRCP showed a round dark signal of a large calculus in the GB neck. C. Coronal image demonstrates the relationship between the calculus and common duct (arrow).



Table 4. Miscellaneous Diseases (n= 19)

Disease	Diagnosis	
	Correct	Incorrect
Serous tumor of pancreas	2	-
Mucinous tumor of pancreas	1	-
Mucin hypersecreting tumor of pancreas	3	-
Pseudocyst	1	-
Ampullary benign stricture	1	1
Anomalous pancreaticobiliary duct union & choledochal cyst	1	-
GB empyema	1	-
Adenomyomatosis	2	-
Mirizzi's syndrome	1	-
Recurrent pyogenic cholangitis	4	-
Duodenal diverticulum	1	-

spectively, and diagnostic accuracy was 99.5 % (368/370) (Table 3).

Twelve other miscellaneous diseases and their frequency of diagnostic accuracy are shown in Table 4. A benign stricture of the ampulla of Vater was falsely interpreted as normal. A subtle narrowing of the ampulla of Vater was neglected at the time of interpretation of MR images. The others were correctly interpreted on the basis of the same criteria applied in CT scanning and conventional cholangiopancreatography (Fig. 7).

### Discussion

For the diagnosis of various pancreaticobiliary diseases, different diagnostic modalities such as computed

tomography and sonography have been employed in radiological fields and ERCP in internal medicine. ERCP has been regarded as 'the gold standard' because ductal imaging is essential for the accurate diagnosis of diseases of the pancreatic and biliary tract, in which ductal structure plays a crucial role. However, the risk of procedure-related complications of ERCP has been reported to be 1%-5% (23-25), an outcome mainly related to the invasiveness of the procedure. Since Wallner et al. (7) originally described MR cholangiography, many investigators have used MRCP, with various pulse sequences and advanced techniques, for the diagnosis of pancreaticobiliary diseases. Fast spin-echo techniques have been applied successfully to MRCP (17-22) and have shown a high signal-to-noise and contrast-to-noise



Fig. 7. Adenomyomatosis of gallbladder  
T2-weighted coronal image. Multiple intramural high signal lesions from Rokitansky-Aschoff sinuses (arrows) are well demonstrated in the thickened GB wall.

ratio, reduced susceptibility effects, and reduced motion artifact compared with the initially introduced MRCP technique using gradient-echo sequences (7-10). With fast spin-echo techniques, three-dimensional acquisition with respiratory triggering has the advantage of yielding better-quality MIP reconstruction due to a more isotropic voxel size (19, 20). More recently, half-Fourier single-shot rapid acquisition with a relaxation enhancement (RARE) sequence has been applied to MRCP, and this offers ultrafast acquisition times, low artifact susceptibility, and sequential thin slice capability (1-4).

Regan et al. (4) reported that the presence and level of obstruction was accurately depicted on 100% and 87% of occasions, respectively. A little later, Ichikawa et al. (2) reported that single-shot hybrid RARE could provide consistently higher quality MRCP than FSE and the contrast-enhanced Fourier acquired steady-state technique (CE-FAST) because sequential images by single-shot hybrid RARE minimized respiratory, bowel, and cardiac motion artifacts. Most recently, in a large study of 300 patients, MRCP with the half-Fourier RARE technique was reported by Fulcher et al. (5) to be 100% accurate in determining the presence of pancreaticobiliary disease, the presence and level of biliary obstruction, and obstruction due to bile duct calculi. In the same report, the accuracy of MRCP and MR imaging in determining the presence and level of malignant obstruction was said to be 98.2%. The accuracy they reported in diagnosing pancreaticobiliary diseases using MRCP with FSE or HASTE was higher than in any previous reports.

Among our patients, only two cases of calculi were mismatched with the results of ERCP, which was per-



Fig. 8. Gallstone-Mercedes Benz sign.  
T2-weighted coronal MR image clearly depicts a large gallstone showing the typical 'Mercedes-Benz' sign (arrow).

formed before or after MR imaging. In a retrospective review of MR images of a false negative case of CBD stone side by side with ERCP, neither the signal void structure in the CBD lumen nor the dilated CBD were present in MR images. MR images showed only multiple stones in the patient's left hepatic duct. The possibility that an intrahepatic duct stone spontaneously moved to the CBD at some point during the interval between the time of MR imaging and ERCP, which was performed 22 days after MR imaging, could not be excluded. Three cases of malignancy were falsely interpreted. Among these, one case of distal CBD cancer was correctly diagnosed after the retrospective review of MR images, but in two cases of pancreatic cancer, this review did not lead to correct diagnosis. The fact that pancreatic cancers were not detected in MR images suggested that the slightly different signal intensity of the suspicious lesion from that of surrounding normal parenchyma of the pancreas, was not enough to accurately diagnose or even detect a pancreatic mass which was not accompanied by ductal abnormality or mass effect. Additional contrast-enhanced cross-sectional images would have been necessary for correct diagnosis of these cases. In diagnosing malignancy, the small difference in the accuracy of MRCP between our results and those of Fulcher et al. (5) can be explained by the fact that they used conventional cross-sectional MR images including contrast-enhanced T1-weighted images in addition to MRCP in diagnosing suspicious malignancy. Conventional cross-sectional MR imaging with T1-weighted imaging and contrast enhancement does not, however, allow a definite conclusion regarding its rou-

tine use for suspicious pancreatic malignancy.

We added relatively short TE multislice imaging using SSFSE sequencing without fat suppression as in the case of conventional fast spin-echo T2-weighted imaging. This is in contrast to long TE multislice imaging with fat suppression used for MIP reconstruction. For tissue characterization, T2-weighted imaging with relatively short TE and without fat suppression was more informative than source imaging for MIP, and small stones were detected no less accurately. Small stones in the gallbladder or biliary duct which were not detected or incompletely seen on MIP or single projection images, were clearly visualized on T2-weighted axial or coronal images. In view of the limitations of MRCP, short-T2 material in the lumen of bile ducts cannot be easily differentiated from a true stone or other obstructive lesions. This is a consequence of water imaging with only bright or dark signals permitted, which resembles a direct cholangiogram in that a lesion is shown only as a filling defect regardless of its nature. For example, Mirizzi syndrome (Fig. 6) was dramatically depicted on T2-weighted images without fat suppression, showing irregular GB wall thickening with a dark calcified stone impacted in the neck of the gallbladder and compressed mid-common duct without evidence of malignancy in surrounding tissue. MIP and multislice source images showed only bright lumen of CBD and GB, with focal narrowing and round filling defect, respectively. T2-weighted images showed more detailed characteristics of the stone, such as the Mercedes-Benz sign, suggesting the presence of a cholesterol stone in another case (Fig. 8). CNR is superior in MRCP with fat suppression, but CNR is not so critically decreased in T2-weighted images without fat suppression that the lesion can be detected and characterized. Additionally, T2-weighted images could be acquired in a reasonably short period of time, usually less than 20 seconds using SSFSE sequencing, during which time most patients were able to hold their breath. T2-weighted images showed more detailed characteristics of stone and provided more information with which definite masses could be demonstrated and the extension of most malignancies evaluated. T2-weighted images were helpful for determining subsequent diagnostic steps, such as further MR imaging with contrast enhancement or angiography with a more confident impression of malignancy, as well as endoscopic biopsy for tissue confirmation in cases of suspected malignancy without possible delay for other diagnostic outcomes. In addition, the use of T2-weighted im-

ages facilitates decision making with regard to the determination of stone management, medical treatment, surgical removal, or endoscopic extraction.

However, small side branches of the pancreatic duct, if not dilated, could not be clearly evaluated with all SSFSE sequences, though some studies (5, 13) have shown that MRCP can detect small ducts and stones as small as 2mm in diameter. With advance in MR equipment and technology, improvements in spatial resolution are expected. In our study, postsurgical biliary-enteric anatomic change (26) or susceptibility artifact from surgical material was not the cause of false interpretation of MRCP and T2-weighted images. In fact, only one case of CBD stone seen on MR images, which was mismatched with a negative result in ERCP, might be explained by certain reported pitfalls mimicking choledocholithiasis (27). In this case, unfortunately, no further attempt was made to confirm any pathologic condition or artifact (Fig. 4).

In spite of the high accuracy of MRCP in detecting the presence and level of biliary obstruction by calculi, it cannot easily replace ERCP because of the crucial advantage this has as the means of providing simultaneous treatment at the time of diagnosis. Another advantage of ERCP is its role in facilitating biopsy in an equivocal case, particularly in ampullary lesions. In terms of non-invasiveness, however, MRCP can replace ERCP if a therapeutic procedure is not anticipated, and procedure-related mortality and morbidity can thus be avoided. Soto et al. (12) reported that MRCP played an important role in the care of patients in whom ERCP was unsuccessful, or incomplete, or when technical difficulties could be anticipated.

In conclusion, MR cholangiography with MIP or a single projection technique is an accurate method for diagnosing various pancreaticobiliary diseases with high specificity and sensitivity while bearing in mind the need for a therapeutic procedure and resultant cost-effectiveness. Additional T2-weighted images that can be acquired in a reasonably short time with MRCP would be informative in determining the next step of diagnosis or treatment.

## References

1. Reuther G, Kiefer B, Tuchmann A, Pesendorfer FX. Imaging findings of pancreaticobiliary duct diseases with single-shot MR cholangiopancreatography. *AJR* 1997;168:453-459
2. Ichikawa T, Nitatori T, Hachiya J, Mizutani Y. Breath-held MR cholangiopancreatography with half-averaged single shot hybrid rapid acquisition with relaxation enhancement sequence: compar-

- ison of fast GRE and SE sequences. *J Comput Assist Tomogr* 1996; 20:798-802
3. Miyazaki T, Yamashita Y, Tsuchigame T, Yamamoto H, Urata J, Takahashi M. MR cholangiopancreatography using HASTE(half-Fourier acquisition single-shot turbo spin-echo) sequences. *AJR* 1996;166:1297-1303
  4. Regan F, Smith D, Khazan R, Bohlman M, Schultze-Haakh H, Champion J, et al. MR cholangiography in biliary obstruction using half-Fourier acquisition. *J Comput Assist Tomogr* 1996;20:627-632
  5. Fulcher AS, Turner MA, Capps GW, Zfass AM, Baker KM. Half-Fourier RARE MR cholangiopancreatography: Experience in 300 subjects. *Radiology* 1998; 207:21-32
  6. Yamashita Y, Abe Y, Tang Y, Urata J, Sumi S, Takahashi M. In vitro and clinical studies of image acquisition in breath-hold MR cholangiopancreatography: single-shot projection technique versus multislice technique. *AJR* 1997;168:1449-1454
  7. Wallner BK, Schumacher KA, Weidenmaier W, et al. Dilated biliary tract: evaluation with MR cholangiography with a T2-weighted contrast-enhanced fast sequence. *Radiology* 1991;181:805-808
  8. Morimoto K, Shimoi M, Shirakawa T, et al. Biliary obstruction: evaluation with three-dimensional MR cholangiography. *Radiology* 1992;183:578-580
  9. Ishizaki Y, Wakayama T, Okada Y, et al. Magnetic resonance cholangiography for evaluation of obstructive jaundice. *Am J Gastroenterol* 1993;88:2072-2077
  10. Hall-Craggs M, Allen CM, Owens CM, et al. MR cholangiography: clinical evaluation in 40 cases. *Radiology* 1993;189:423-427
  11. Lee MG, Lee HJ, Kim MH, et al. Extrahepatic biliary diseases: 3D MR cholangiopancreatography compared with endoscopic retrograde cholangiopancreatography. *Radiology* 1997;202:663-669
  12. Soto JA, Yucel EK, Barish MA, Chuttani R, Ferrucci JR. MR cholangiopancreatography after unsuccessful or incomplete ERCP. *Radiology* 1996;199:91-98
  13. Becker CD, Grossholz M, Becker M, Mentha G, Peyer R, Terrier F. Choledocholithiasis and bile duct stenosis: diagnostic accuracy of MR cholangiopancreatography. *Radiology* 1997;205:523-530
  14. Barish MA, Soto JA, Yucel EK. Magnetic resonance cholangiopancreatography of the biliary ducts: techniques, clinical applications, and limitations. *J Magn Reson Imaging* 1996;8:302-311
  15. Taourel P, Bret PM, Reinhold C, Barkun AN, Atri M. Anatomic variants of the biliary tree: diagnosis with MR cholangiopancreatography. *Radiology* 1996;199:521-527
  16. Guibaud L, Bret PM, Reinhold C, Atri M, Barkun AN. Bile duct obstruction and choledocholithiasis: diagnosis with MR cholangiography. *Radiology* 1995;197:109-115
  17. Reinhold C, Guibaud L, Genin G, Bret PM. MR cholangiopancreatography: comparison between two-dimensional fast spin-echo and three-dimensional gradient-echo. *J Magn Reson Imaging* 1995;5:379-384
  18. Soto JA, Barish MA, Yucel EK, Ferrucci JT. MR cholangiopancreatography: findings on 3D fast spin-echo imaging. *AJR* 1995;165:1397-1401
  19. Barishi MA, Yucel EK, Soto JA, Chuttani R, Ferrucci JT. MR cholangiopancreatography: efficacy of three-dimensional turbo spin-echo technique. *AJR* 1995;165:295-300
  20. Soto JA, Barish MA, Yucel EK, et al. Pancreatic duct: MR cholangiopancreatography with a three-dimensional fast spin-echo technique. *Radiology* 1995;196:459-464
  21. Takehara Y, Ichijo K, Tooyama N, et al. Breath-hold MR cholangiopancreatography with a long-echo-train fast spin-echo sequence and a surface coil in chronic pancreatitis. *Radiology* 1994;192:73-78
  22. Low RN, Sigeti JS, Francis IR, et al. Evaluation of malignant biliary obstruction: efficacy of fast multiplanar spoiled gradient-recalled MR imaging vs spin-echo MR imaging, CT, and cholangiography. *AJR* 1994;162:315-323
  23. Bilbao MK, Dotter CT, Lee TG, Katon RM. Complications of endoscopic retrograde cholangiopancreatography(ERCP): a study of 10,000 cases. *Gastroenterology* 1976; 70: 314-320
  24. Hamilton I, Lintott DJ, Rothwell J, Axon ATR. Acute pancreatitis following endoscopic retrograde cholangiopancreatography. *Clin Radiol* 1983; 34:543-546
  25. Thoeni RF, Fel SC, Goldberg HI. CT detection of asymptomatic pancreatitis following ERCP. *Gastrointerst Radiol* 1990; 15:291-295
  26. Pavone P, Laghi A, Catalano C, et al. MR cholangiography in the examination of patients with biliary-enteric anastomoses. *AJR* 1997; 169:807-811
  27. David V, Reinhold C, Hochman M, et al. Pitfalls in the interpretation of MR cholangiopancreatography. *AJR* 1998;170:1055-1059

